



Report High IWC detection scheme evaluation against in situ measurements

Project Number	ACP2-GA-2012-314314		
Project Title	High Altitude Ice Crystals		
Abstract¹	To write.		
Due date	01/01/2014	Actual submission date	DD/MM/YYYY
Nature²	R + O		
Document identifier	HAIC_WP33_D33.3_R0.1.doc		

Deliverables' contributors³

Deliverable Leader	E. Defer/CNRS/WP33 leader			
Contributors	M. Faivre/CNRS/WP33 participant E. Defer/CNRS/WP33 leader			
Internal Reviewers	Name/Beneficiary short name/Role in project			
Process Auditor	Name/Beneficiary short name/Role in project			
Deliverable Status	X	Draft	In Review	Released
Comments				
Dissemination Level⁴	CO			

¹ An abstract is mandatory

² R = Report; R+O = Report plus Other. Note, all "O" deliverables must be accompanied by a deliverable report.

³ Refer to the HAIC Management Handbook for more details on the Deliverable Process and roles of contributors.

⁴ RE = Restricted to a group specified by the consortium (including the Commission Services), PP = Restricted to other programme participants (including the Commission Services), CO = Confidential, only for members of the consortium (including the Commission Services), PU = Public

Table of contents

1	6	
2	Introduction	7
3	The detection of high IWC clouds from GEO MTSAT and airborne instrument	7
3.1	The MTSAT sensors	7
3.2	The RASTA sensor.....	7
4	Data material making of	8
4.1	The HAIC 2014 Darwin campaign	8
4.2	Data preparation : Build ascii file	8
4.2	Forecast IWP from set of radiances : Algorithm	8
4.3	RASTA_MTSAT_NNET	8
4.4	Exploring TRMM observations during the HAIC 2014 Darwin research flights	11
4.3.1	<i>Flight #1</i>	11
4.3.2	<i>Flight #2</i>	12
4.3.3	<i>Flight #3</i>	12
4.3.4	<i>Flight #5</i>	12
4.3.5	<i>Flight #6</i>	12
4.3.6	<i>Flight #7</i>	22
4.3.7	<i>Flight #11</i>	22
4.3.8	<i>Flight #14</i>	22
4.3.9	<i>Flight #15</i>	22
4.3.10	<i>Flight #16</i>	23
4.3.11	<i>Flight #19</i>	23
4.3.12	<i>Flight #21</i>	23
4.4	Investigating past AIRBUS campaigns	23
5	Conclusion.....	23
6	References	23

List of figures

Figure 1-1	99
Figure 1-2	9
Figure1	21-23
Figure4	23
Figure3	21-23
Figure4	23
Figure5	24
Figure6	24
Figure7	24
Figure8	25
Figure9	25
Figure10	25
Figure11	26
Figure12	26
Figure13	27
Figure14	27
Figure15	28
Figure16	28
Figure17	29
Figure18	29
Figure19	29
Figure20	30
Figure21	30

List of tables

Erreur ! Aucune entrée de table d'illustration n'a été trouvée.

List of acronyms / abbreviations used in this document

Acronym / abbreviation	Definition
AMSRE	Advanced Microwave Scanning Radiometer – EOS
BTD	Brightness Temperature Difference
CALIOP	Cloud-Aerosol Lidar with Orthogonal Polarization
CALIPSO	Cloud-Aerosol Lidar and Infrared Pathfinder Satellite Observations
CPR	Cloud Profiling Radar
DARDAR	(LATMOS)
DJF	December-January-February
DoW	Description of Work
GEO	Geostationary Earth Orbit
GOES	Geostationary Operational Environmental Satellite
HAIC-ISDB	HAIC In-service event Satellite Database
GMT	Greenwich Meridian Time
HAIC	High Altitude Ice Crystals
IR	Infrared
JJA	June-July-August
LEO	Low Earth Orbit
LT	Local Time
MAM	March-April-May
MODIS	Moderate Resolution Imaging Spectroradiometer
MOZAIC	airborne in-situ measurements for ozone, water vapor, carbon monoxide, and total nitrogen oxides (NOy). Measurements are geo-localized (latitude, longitude and pressure) and come with meteorological observations (wind direction and force, temperature). Data acquisition is automatically performed during round-trip international flights (ascent, descent and cruise phases) from Europe to America, Africa, Middle East, and Asia.
MSG	Meteosat Second Generation
MTSAT	Multi-functional Transport Satellite
MW	Microwave
NCAR	National Center for Atmospheric Research
NH	North Hemisphere

PARASOL	Polarization & Anisotropy of Reflectances for Atmospheric Sciences coupled with Observations from a Lidar
RASTA	Radar Aéroporté et Sol de Télédétection des propriétés nuAgeuses
Robust Probe	
RDT	Rapid developing Thunderstorm (MétéoFrance)
SEVIRI	Spinning Enhanced Visible and Infrared Imager
SH	South Hemisphere
SON	September-October-November
TRMM	Tropical Rainfall Measurement Mission (NASA+JAXA)
TWC	Total Water Content measured by a robust probe
VIS	Visible
RMnnet	Rasta-Mtsat neural network for Darwin observations

Glossary of terms used in this document

Term	Definition
Brightness temperature	
Cloud cover	
Optical thickness	
Oxygen pressure	
Rayleigh pressure	
Spherical albedo	
Thermodynamic phase	
Visible composite	

1 Executive summary

Work at Lerma UMR8112 on HAIC project

As a contractor Research Engineer at LERMA, being funded on a HAIC grant covering the period Sep.2014-Aug.2015, I worked on several issues related to LEO and GEO observations, in the scope of SP3/WP3.3. The work is directed by Dr Eric Defer who is the SP3 leader. Most of the analyses I developed are related to the 2014-Darwin campaign. Five sets of Observations and Models have been explored, analyzed or compared with each other :

Table 3. Instrument and model databases used

Instrument name/ owner	Instrument	Type/ Campaign	Database Format/size	Quantities	Work
1) RASTA (Cnes)	Radar 95 GHz	Airborne Darwin'14 Cayenne'15	netcdf 5GB	IWC profiles → IWP above 9km	a) tracks on MTSAT b) density/IWP/ratio BT/IR bins c) nnet
2) MTSAT (Jaxa)	Radiometer 10.8,12,6.8μm	GEO Cayenne'15	netcdf 50GB	Radiances/BT	Along with 1) for NNET making
3) AMSRE TRMM (Nasa – Jaxa)	MW sounder 89GHz	LEO Darwin'14		BT	NNET comparison
4) MOZAIC-IAGOS		Airborne	Ascii	Air-speed Static-T	Cumulated 2008 flight tracks
5) DARDAR (Latmos)	Cloudsat Radar & Caliop Lidar fusion	LEO Darwin'14 Cayenne'15	Hdf5	Reflectivity, depolarisation IWC	
6) RDT (MTF)		Model Darwin'14 Cayenne'15	Ascii	Contour cells	NNET comparison

NB : A-train data were not used here owing to a lack of space/time matching during 2014-Darwin campaign.

The main part of the work led at LERMA is the neural network development for IWP assessment from radiance measurements. Cross-comparisons were performed between the detection tool developed at Lerma and BT-maps measured by LEO Nasa-Jaxa TRMM MW sounder at 89GHz. In addition to NNET vs LEO MW observation comparisons, Nowcasting detection tool from MeteoFrance (RDT) was also solicited for case study comparisons.

The five technical and scientific topics I worked on over the past eight months are :

- IWP and observation density Distributions in radiance and BT domains for Darwin 2014-campaign [*Fig.3*]
- MTSAT-RASTA Neural network package for automated HIWP cells detection [*Figs4-8*]
- Case study HIWP neural network-nowcasting-observation comparisons [*Fig.9*]
- MOZAIC-AGOS Dataset
- CAYENNE data fusion support

2 Introduction

Remote sensing instruments can characterize cloud properties. Space-based remote sensing offers the possibility to document clouds over sea and land though LEO and GEO missions. According to the type of orbits and mission applications, different instruments operating at different wavelengths (visible, infrared, microwave) and different principles (active versus passive).

This documents aims to present work performed at LERMA, during the period September 2014 to May 2015, as a HAIC contract Data Engineer. The main duties that were addressed are :

- (i) To develop an analysis package for the Darwin 2014 campaign
- (ii) To provide “back-office” support for Cayenne 2015 campaign
- (iii) To write technical reports accordingly and participate to monthly telecons and SP3 meetings as well

3 The detection of high IWC clouds from MTSAT radiances and RASTA IWCs

3.1 MTSAT_RASTA_NeuralNET Algorithm and Matlab Code

The main scientific goal here is to retrieve qualitative and possibly quantitative information on IWP levels inside or at vicinity of cloud cells. The approach is to estimate IWP levels from IR and WV radiances by using a supervised learning method. HIWP locations can be either associated with convective cells or stratiform clouds.

The technical challenge to achieve this scientific purpose is to properly design a robust and accurate neural-network. First of all, a bench of preprocessings must be employed prior to the network itself.

The analysis relies and fits on the Darwin Campaign held on January and February 2014, in Northern Australia. Thus, the analysis is fully dependent on this database. Owing to the specific tuning, this means the package parametrizations may not apply straightforwardly to another database. The first instrument is the RASTA radar on-board of Falcon20. It measures reflectivity profiles in both Nadir and Zenith directions. IWC profiles are derived from reflectivity profiles under the assumption of same prevalent microphysical properties over the cloud depth [*Paper ref J.-F. Gayet*]. In addition to the airborne measurements, we also take advantage of GEO satellite MTSAT passive optics

observations. The satellite operated by JAXA provides four radiances at 10.8, 12.0, 6.8 μm as infrared channels and 3.8 μm for the water vapour channel. It also provides a VIS channel, but we did not make use of it in our study.

The code package is developed in Matlab R2012b. It is modular and the package benefits from a parametrization bash script which launches the main code. Calculation time on a 128 Gbytes, AMD 2.1 GHz machine is roughly 5 minutes for the whole process over a $10 \times 10^\circ$ lat-lon area. The package is not parallelized in regards to short computation time. The package's kernel really is the design and configuration of the neural network itself. This is presented in further details in section §3.3.

The neural network is expected to detect IWP levels above 2kg/m^2 with a Probability Of Detection beyond 60% and a False alarm rate under 20%. Bias remains above 80% [Fig.10].

The milestones for building a robust and reliable neural network are the following :

- Data preparation and processing (collocation, time delay, parallax correction, log)
- Adapted Neural network type for handling classification problem
- Proper neural network tuning : type, configuration (number of IWP levels, IWP level ranges setup, number of hidden layer neurones, transfer function, output function, input data preprocessing)
- Quality criteria fulfilment (§3.2.5)
- Retrieved HIWP flagmaps being recurrently consistent with other observations and nowcasting models
- 2D-outputs shall avoid background artefacts (IWP level < 2kg/m^2)
- 2D-outputs shall succeed to identify HIWP areas (IWP level > 4.5kg/m^2) vs MTSAT Low Radiances in channel 1

Explicit Neural Network uncertainties are not calculated in this package. Nevertheless, confidence intervals are calculated for each IWP level based on the training part and box plots statistics are performed for each IWP level. More details and a figure are given in section § 3.2.2.

The Neural network is a feedforward type. It consists first in an input layer grouping the four MTSAT radiances. Then, the input layer connects to a hidden layer which has N neurones coupled with an aggregation and a transfer functions. Finally, the output layer corresponds to the IWP levels retrieved after passing through a handmade output function. Since we are dealing with a classification problem, the selected Matlab function is "Patternnet". As per Matlab Machine Learning package advises, this routine is indeed highly recommended when addressing classification topic.

NB : other nnet functions were actually tested, but with less success.

Two setups give similar results for IWP up to 5kg/m^2 and both are reproducible from one MTSAT image to the other [Doc. Synthese_NNET_Mai2015]. Roughly 20 MTSAT domains were tested over different Darwin campaign dates.

NEURAL NETWORK configuration :

- The training function is “Scaled Conjugate Gradient”. The transfer function is the sigmoid
- 5 hidden layers with respective number of neurones 14, 12, 10, 8, 6
- function applied to Inputs : RADS → sqrt(RADS+epsilon)
- function applied to targets : IWP → log(IWP+epsilon)
- Output function : $Y = \begin{cases} \text{round}(Y - 0.2), & \text{IWP} < 4.5\text{kg/m}^2 \\ \text{round}(Y + 0.6), & \text{IWP} \geq 4.5\text{kg/m}^2 \end{cases}$
- A posteriori correction is finally applied to each pixel of inconsistent IWP_level wr Radiance 1

→ Configuration #2 is the reference one due to a better one-dimension fitting vs IWP_level_Target. Both configurations give almost always the same location and size for HIWP cells. Though, Config#2 retrieves higher IWP_level values. Moreover, its empirical cumulated distribution function (CDF) is closer to target's CDF one than with config#2. Consequently, config#2 is the one being recommended and used in the figures presented. However, one has to be aware that in a few rare cases, a posteriori IWP_level pixel correction vs Rad10.8 level is needed in configuration#2, whereas no such correction is needed with the first setup.

3.1.1 Darwin'2014 campaign

Here are the Data preparation steps which lead to create a unique ascii file with all the RASTA+MTSAT netcdf required contents :

- 1) IWC profiles are provided by Airborne RASTA on-board Falcon20 observations
- 2) MTSAT Rad1 to 4 parallax and time delay corrections
- 3) IWP = sum(IWC_level(n)*thickness_level(n) | altitude_level(n)>=9km)
- 4) IWP are summed up over colocated each MTSAT pixel

The resulting global ascii file has 29,000 rows.

Table 4. Level1 statistics of Radiances and IWP cumulated beyond 9km

	Min	Max	Mean	Q1	median	Q3
Radiance 1 10.8 µm	0.52	8.22	1.64	0.89	1.22	1.9
Radiance 2 12 µm	0.66	7.22	1.74	1.36	1.04	2.04
Radiance 3 6.8 µm	0.09	1.26	0.36	0.17	0.27	0.47
Radiance 4 3.8 µm	0.001	0.6	0.06	0.03	0.04	0.06
IWP for height ≥ 9km	0	32.7 kg/m ²	kg/m ²	0.13	0.81	2.77

Data Preprocessing

Before starting neural network calculations, prior dataset processings are required.

a- Data cleaning

First, data cleaning is applied. The filtering we used only consists in removing invalid points. No a priori filtering was used for our input database.

b- IWP collocation in MTSAT pixels

Then, IWP values are summed up over MTSAT pixels. This operation is performed taking into account again the parallax effect in MSAT image. The input file stores RASTA IWP integrated values above 9 km.

c- IWP spectral distribution

Next, the IWP distribution is modified to compensate the sharp decay in IWP number of points beyond 2kg/m^2 [Fig.12]. IWP array is then sorted in increasing order and other arrays are sorted accordingly. Input data distributions are summarized in individual boxplot.

Neural Network performances and training checking

Several performance and consistency assessment tools are provided in the package :

- Boxplots IWPLevels Outputs vs IWPLevels Targets
- Boxplot difference IWPLevels Output – Targets
- Empirical Cumulated Density Function Output vs Target IWP levels
- Probability of Detection False Alarm Ratio, Bias
- Conditionnal radiance histogram vs IWP value
- Performance curve and convergence iteration number

The Neural network satisfies convergence conditions after about 500 iterations. Figures 11 to 13 show verifications # listed above on training performances.

3.1.2 Simulation Result Checking Tools

Several verification tools for assessing Neural-network results quality are designed. The first one is the plotting of IWP_level_Output boxplots with respect to IWP_level_Target. It give us information about the output distribution per target reference. The overall (IWP_lev_target,IWP_lev_output) boxplot is also plotted. Besides Target/Output training consistency, the other quality tool is the testing set simulation. 15% of the database was allocated for testing purpose, i.e. these are datapoints not used in the training process. They are kept aside in order to apply the trained nnet onto them afterwards. The remaining 15% are used for validation.

3.1.3 A supervised learning package has been developped to retrieve IWP classes from radiance measurements

Based on literature and technical discussion groups, I selected a supervised learning approach for our problem of HIWP levels retrieval. Other methods like k-means, clustering or svm were not explored.

Package NEURALNET =

- 1) 1 directory Ascii INPUTS + 1 Dir for MTSAT netcdf files
- 2) 1 bash for manual ROI and date+time

- 3) 1 bash for automated ROI +/- 1° around RASTA track
- 4) 1 Matlab MAIN, 1 subMAIN for training part
- 5) 1 subMAIN for simulation part
- 6) 1 TOOLS directory with 24 routines & 1 subdirectory dedicated to NNETsetup routines
- 7) 1 Output dir for eps figures

Algorithm to retrieve IWP classes from four radiances using a 1-hidden layer, feedforward neural network :

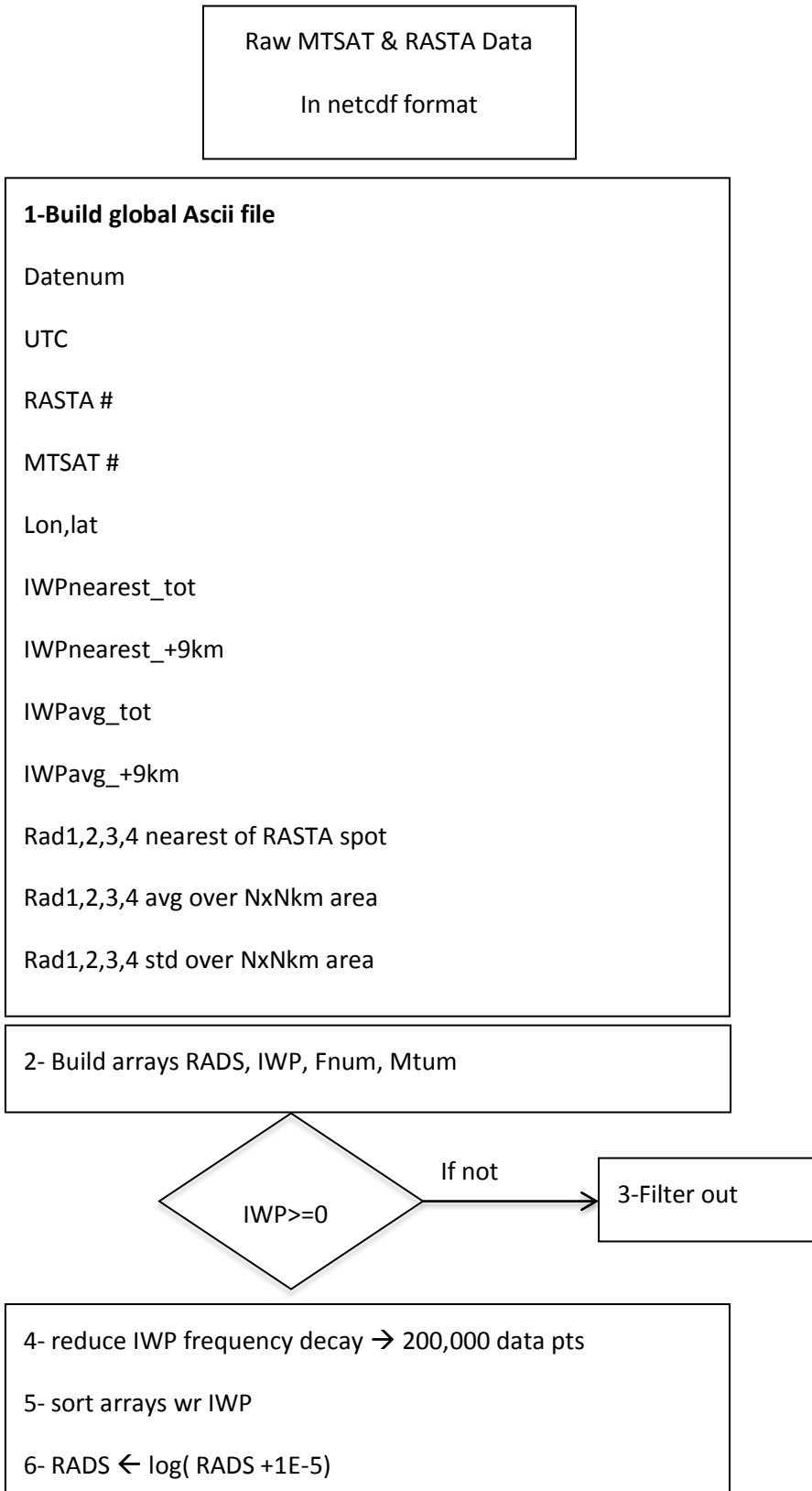
- 1) read global Ascii compiling 19 flight data : date, time, lon, lat, IWPTot, IWP, Rad1,2,3,4
- 2) build arrays for IWP, RAD1,2,3,4, Rasta Fnumber, MTSAT Mnumber
- 3) pre-process training_set : reduce frequency decay as IWP increases
- 4) pre-process the data : sort arrays wr IWP
- 5) pre-process the data : RADS $\leftarrow \log(RADS + 1E-5)$ | channels 1,2,3,4
- 6) build IWP class array : 6 classes = [0-0.6;0.6-1.7;1.7-3;3-4.5;4.5-6.4;6.4-40]kg/m²
- 7) build neural network using Matlab “Patternnet” designed for Classification problems
- 8) use 1 hidden layer with N=3 neurones : 4Input neurones * 3HL neurones > 6OUT neurones
- 9) Output fcn : $Y \leftarrow [Y + alpha*(Y-Yp)/(Nbcla-Yp)]$; where Y is a IWP class in 0:5, Yp=4, Nbcla=6
- 10) run the experiment over one or several cases with ./bash_NNETcode.sh
- 11) product types : (i) boxplot IWPcl Out-Target, (ii) scatterplot in log10 scale Out vs Target, (iii) 1D RASTA track IWPcl Out& Target, (iv) 2D MTSAT image with IWPcl

Quality criteria of NNET :

- (i) NBI*NBHL > NBO
- (ii) Boxplot(O-T) ok
- (iii) no artefacts
- (iv) 1D trainingfit
- (v) CDF_O ~ CDF_T
- (vi) 2D cell detection efficiency vs MTSAT R1 image
- (vii) 2D detection and stability over a range of shapes of HIWP areas : rounded, patches, branches and other patterns

Neural network Scheme I/HL/FCNS/O

Algorithm Flow chart



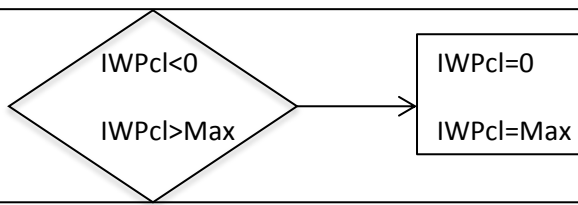
7- Build IWP classes [0-0.6-1.7-3-4.5-6.4-40]kg/m²

8- Build Neural network = Patternet(3)

- ➔ trainFcn = 'LM' Levenberg-Marquardt
- ➔ nb Hidden layer = 1 / nb neurones = 3
- ➔ data set splitting : 70% training, 15% validation, 15% testing
- ➔ 6 IWPcl as output
- ➔ empirical output fcn :


```
set1=find(IWP>=4.5kg/m2); IWPcl(set1) ← round(IWPcl(set1)+0.8)
set2=find(IWP<4.5kg/m2); IWPcl(set2) ← round(IWPcl(set2)-0.5)

This Outputfcn enables to get a CDF_output very close from
CDF_target
```



9- Nnet convergence at 500 iterations

10- NeuralNetwork simulations for IWP class masks over MTSAT ROIs

APPLY DOWNSCALING : number of IWPllevel groups = 4
0-1; 1-3; 3-6; 6-40 kg/m²

Makes Histos diffs Output - Target on Downscaled IWP groups
Make 1D series Output and Target based on downscalled groups

Package Implementation in Matlab R2012b

The Matlab package is decomposed in reading, calculation, testing, plotting

- a. Read ascii file with RASTA&MTSAT 1D records
- b. Extract arrays : IWP, RADS1,2,3,4, Fnumvect, MTnumvect, date time
- c. Define neuralnetwork : type from Matlab machine learning library, training function = scale-conjugated gradient,
- d. Read netcdf file MTSAT image and record Pixel radiances

- e. Use trained network with IWPmask = sim(RADS)

Neural Network strengths and weaknesses

The MTSAT-RASTA NNET has proven its capability to identify geographical areas having High IWP levels. In a systematic way, in respect to a bench of case study, the areas detected by the neural network occur to be quite in good agreement with MTSAT 10.8 μm radiance. Static thresholding applied to MTSAT image (Figs. 5-10) demonstrates clear correspondance between observation and detection tool. Cross-comparisons involving observations and nowcasting tool do indicate the nnet has robustness in locating critical areas, as demonstrated to the extent of 20 case study (Figs. 5-10,14-21). Nevertheless, it has to be mentioned that 1D fitting of IWP targets is not perfect, though being fairly consistent, as indicated in boxplot per IWP level (Fig.12). Discrepancies between Outputs and Targets may relate to a lack of filtering in the input data. Occurrence of local discrepancies are partly due to outliers in the database, when low radiances are associated with low IWP or the opposite way. Yet, when considering meta IWP classes : Low IWP ($<1\text{kg.m}^{-2}$), Medium to High IWP (1 to 5kg.m^{-2}) and very High IWP ($>5\text{kg.m}^{-2}$), it is shown that differences between Target and Output remain low. Indeed, the distributions of difference T-O are properly centered onto null difference in median for the configuration with 6 classes and Levenberg-Marquardt transfer function.

Downscaling is finally applied onto IWP levels : four “IWP meta-classes” are kept which are as following :

Group1 : 0-1kg.m⁻²; group2 : 1-3kg.m⁻² ; group3 : 3-6kg.m⁻² ; group4 : 6+ kg.m⁻²

4 Neural Network Outputs vs data and model sets

Three cross-comparison experiments were undertaken. Two of them are made using GEO (MTSAT) and LEO (TRMM) passive optics observations. The third one is relative to the operational nowcasting tool developped by MeteoFrance, RDT. Likewise, we are expecting soon to make comparison with operational nowcasting tool HIWC from KNMI.

4.1 Nnet vs MTSAT Radiance 10.8 μm

Figs.5-9 show some examples of straightforward comparisons between Nnet cells plotted on specific ROIs and corresponding MTSAT thresholded Radiance channel#1 image. It is reasonable to say that all studied cases show very similar results for observed and retrieved HIWP/low radiances($R1<1.25\text{W.m}^{-2.\text{sr}}^{-1}$) cells. These results regarding 2D-maps in IWPlevels abnd Radiance 10.8 mc levels tend to indicate a good generalization capability for the trained network. By doing so, it fulfills conditions (iii), (vi) and (vii) of nnet quality criteria listed in section § 3.1.5.

4.2 Nnet vs AMSRE-TRMM MW 89GHz

The second set of side-by-side comparison is relative to LEO TRMM BT measurements. Figs.14 to 18 show the nnet cell detection results vs MTSAT and TRMM BT images. Comparison with TRMM BT indicates comparable features though the timing may not be exactly the same.

4.3 Nnet vs RDT cells

We started assessing NNET behavior in repect of MeteoFrance nowcasting tool : Rapid Developping Thunderstorms (RDT). We made a few case study comparisons in terms of cell expansion and location. The results are shown in Fig.14. They indicate a noticeable matching for most of larger cells. Yet, discrepancies occur in some areas where both MTSAT and nnet do find significant cells, whereas RDT detects far smaller ones. For instance, in Fig14 at . The opposite situation occurs also. Tested flights are F06 and F02. More comparisons are planned to be performed soon.

5 Summary and conclusion

WorkPackage#1 : Darwin 2014 Campaign – status : completed

WP1.A : Neural Network

Darwin 2014-campaign enabled us to build an automated detection tool based on a supervised learning method. The scheme makes use of simultaneous and colocated airborne and GEO observations. The purpose of the network is to retrieve IWP levels from four radiances in IR and WV channels. Core of the analysis relies on proper setup and fine tunning of the neural network function specifically designed for classification problem. Owing to specific focus on airplane cruising altitudes, we decided to integrate IWC from 9km in order to calculate IWP. Prior to analysis, the original database goes through two modifications. The first one is the IWP distribution high value enhancement in order to counter steep decline in IWP frequency for higher values. The second one is the log transform of radiances. The training phase enables to optimize the weight function applied to each neurone layer from input to hidden layer and from hidden to output. Finally, a by-hand designed output function is used to improve the result quality in terms of empirical cumulated distribution function target vs Outputs and box-plot and histograms of differences.

Retrieved IWP cells, i.e. above 2kg.m^{-2} , are compared with thresholded $10.8\mu\text{m}$ radiance over ROIs of about 10° wide in longitude and latitude. In respect to IWPllevel-maps, NNET shows a robust behavior in cell detection over a wide range of patterns. Identified cells and HIWP levels are also positively compared with AMSRE-TRMM MW 89GHz sounder BT maps over 15 examples. HIWP cell shape and size matching are in most cases conclusive enough for BT-IWP comparisons, and very conclusive for Rad10.8-IWP comparisons. As for RDT-Nnet assessment, more comparisons need to be made.

WP1.B : 2D distributions I IWP and density points

Two-dimensional distributions for IWP and density points in radiance and BT domains are plotted since they are useful for synthetic analysis. For instance, it matters to know where the RASTA observations are made wr the overall MTSAT spectral observations. Two modes were operated, either the cumulation of quantities per each flight, or the cumulation over the full campaign (F03, 17-

19 missing). Figures 1 to 3 show examples of distributions in density, density ratio and IWP in BT-domains. The first set of plots are the observation density maps in BT-domains, with a bin of 3.8K (i) for MTSAT full image and (ii) restricted to RASTA spot locations. This shows that relative highest density area correspond to BT less than 200K for BT1-3 (fig.3c). The second set is the same, but using IR binned domains. 36 millions MTSAT points are counted overall. Then, average IWP over RASTA tracks, as well as mean, max, min, sigma IWP are projected in the BT and IR domains. A total of 29,000 data points is reached using RASTA spots over 20 flights.

WorkPackage#2 : Cayenne 2015 Campaign – status : undergoing

We also contributed as “back-office” support for the HAIC-HIWP Campaign organized in Cayenne from May 10th to 29th. Three planes equipped with in-situ probes and nadir/zenith active instruments as well, were flying jointly, at different heights : Falcon20, Convair, Boeing. Additionally, the measurement area takes place within the West side of MSG-Seviri field-of-view. Occasionally, LEO, such as Cloudsat, overpass can occur at proper space-time collocation wr to planes positions and HIWP cells. Our responsibility in this context consisted in post-analyzing Falcon 20 Robust Probe TWC, Rasta Radar IWC and MSG-SEVIRI GEO scanning radiometer radiances. First, MSG-SEVIRI 10.8mc images focused on the region of interest are plotted with F20 flight overlapped. Then, time series of F20, Convair and Boeing altitude, TWC and IWC are systematically plotted through the database. In addition, we are also investigating possible relationships between TWC (resp. IWC) and 10.8 mc radiance, by adapting the neural network designed from Darwin campaign.

WorkPackage#3 : MOZAIC-AGOS – status : undergoing

Preliminary work was started regarding MOZAIC-AGOS flights using Air-Speed and Static-Temperature parameters. Extraction of peaks vs average signal using a Savitzki-Golay smoothing is applied to Static Temperature and Air Speed times series. Peaks and their lat,lon,UTC are saved in ascii files.

As a conclusion regarding the work during the HAIC contract as a data engineer, first I would like to say I am honoured to have participated, even at a very modest level, to such an ambitious and critical project. HAIC has both industrial and scientific dimensions and it is very exciting to work in its aim. Hopefully, the work developed in the frame of Darwin’s campaign will be adaptative to other airplane observation campaigns, and firstly to Cayenne 2015. In this purpose, i started to make the necessary adjustments that will enable next to use the tools for MSG-SEVIRI and Rasta radar on-board of F20 in the frame of the 2015 Cayenne campaign.

6 References

Defer, E., F. Parol, A. Guignard, and J. Delanoë, Database of space-borne observations in areas of pilot reported glaciated icing conditions, HAIC D33.1 report, 2014.

Defer, E., F. Parol, A. Guignard, and J. Delanoë, Database of space-borne observations in areas of pilot reported glaciated icing conditions, HAIC D33.2 report, 2014.

Grandin, A., A. Schwarzenboeck, J. Cammas, and A. Protat, SP2 Progress report at M24, HAIC D21.2 report, 2014.

Meirink, J. F., and J. De Laat, Retrieval of high IWC from MSG-SEVIRI: first algorithm version, HAIC D32.1 report, 2014.

Documents :

Synthese_NNET_Mai2015.pptx

NNET_TRMM_Avril2015.pptx

NNET_RDT_Avril2015.pptx

FIGURES

First set of figures is dedicated to density and IWP distribution in Radiance and BT domains

Figure 1. Density of MTSAT observations wr MTSAT Radiance couples cumulated over Darwin's dataset

Figure 2. same as Fig.1, but restricted to RASTA track locations

Figure 3. Average RASTA IWP(Height \geq 9km) wr MTSAT radiance couples

Figure 4. same as Fig3. wr BT couples

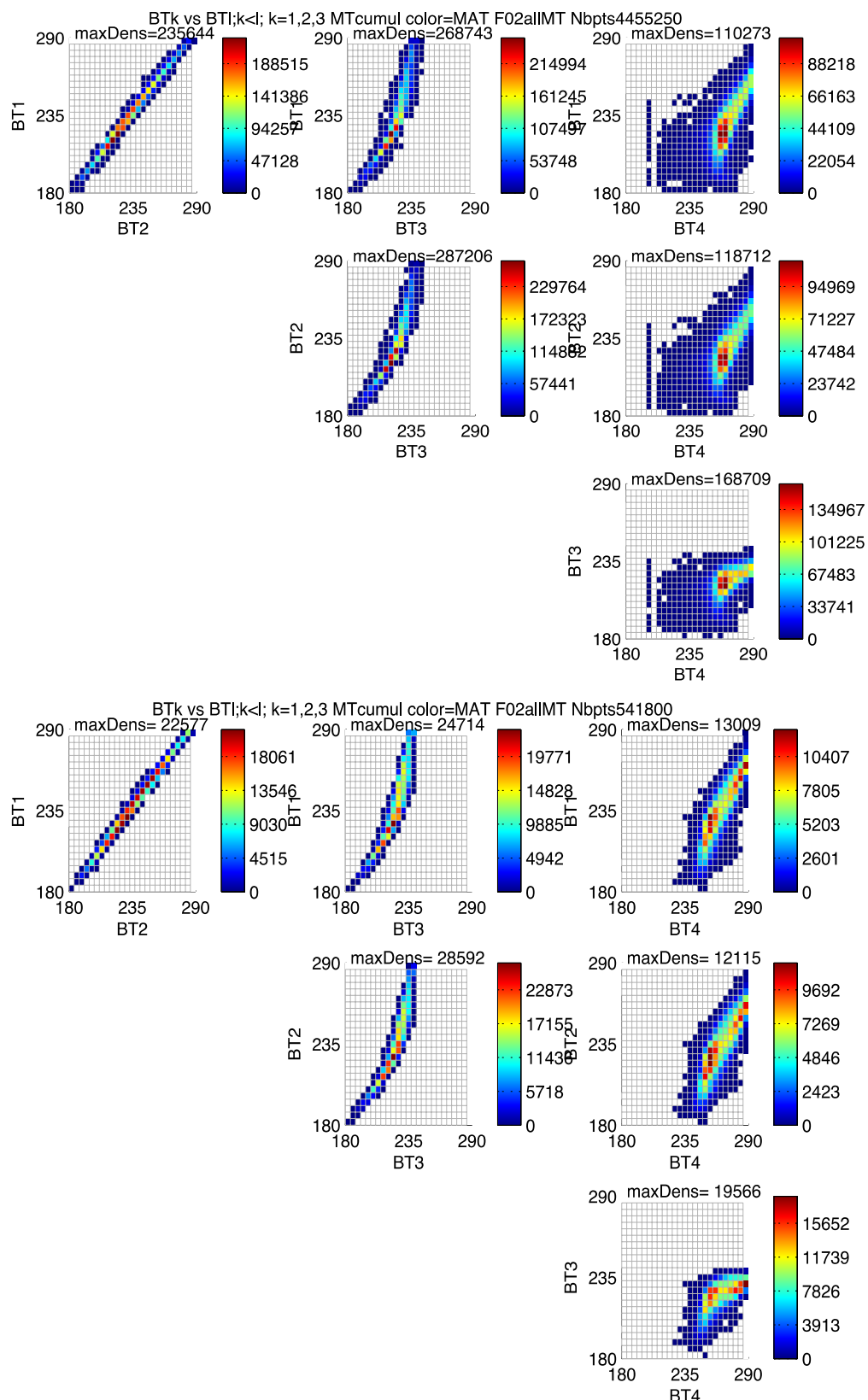


Figure 1. (top) Density map in BT domains for RASTA flight#2 time coverage cumulated over full images. (bottom) Density map in BT restricted to MTSAT pixels intersected by RASTA track. Colors are related to mean density points per BT bin.

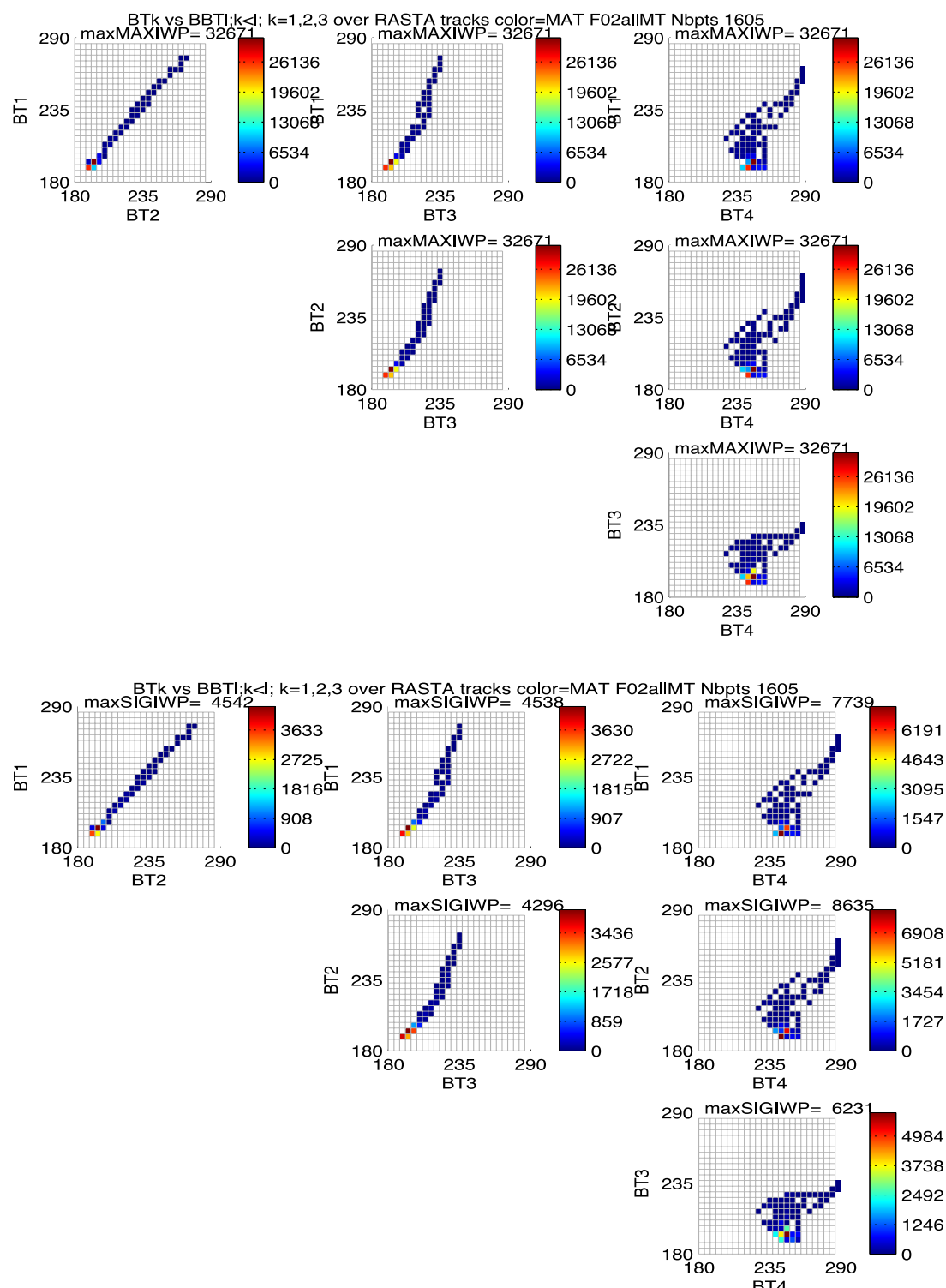
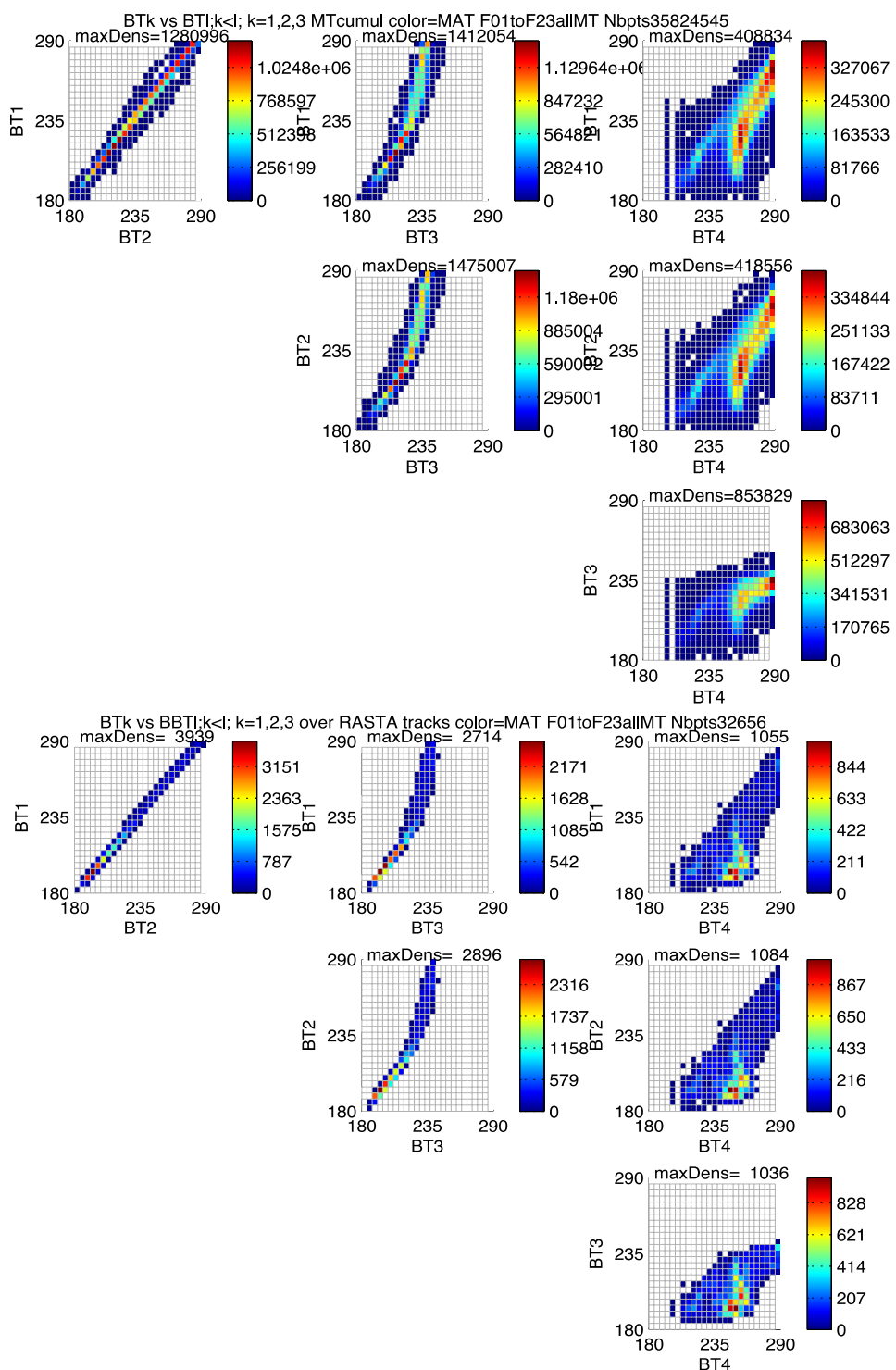


Figure 2. (top) IWP Max map in BT domains for RASTA flight#2 time coverage. (bottom) IWP Min map. IWP max (resp. min) values are averaged by BT bins.

Cumulated 2D distributions over Darwin2014 20 flights : F01,02,04-16,19,22,23

MTSAT Density, RASTA spots density, Average, Min, Max, Variance, in BT I,j; i=1-3 & j=i+k; k=1-3 domains (resp. Irij domains)



Figures3.a, b Density=number of points of (a) MTSAT pixels in BT domains
 (b) RASTA observations in BT domains in linear scale
 Matrix are 25x25 BT bins in the range 180-290K, i.e. a bin is 4.4K wide.

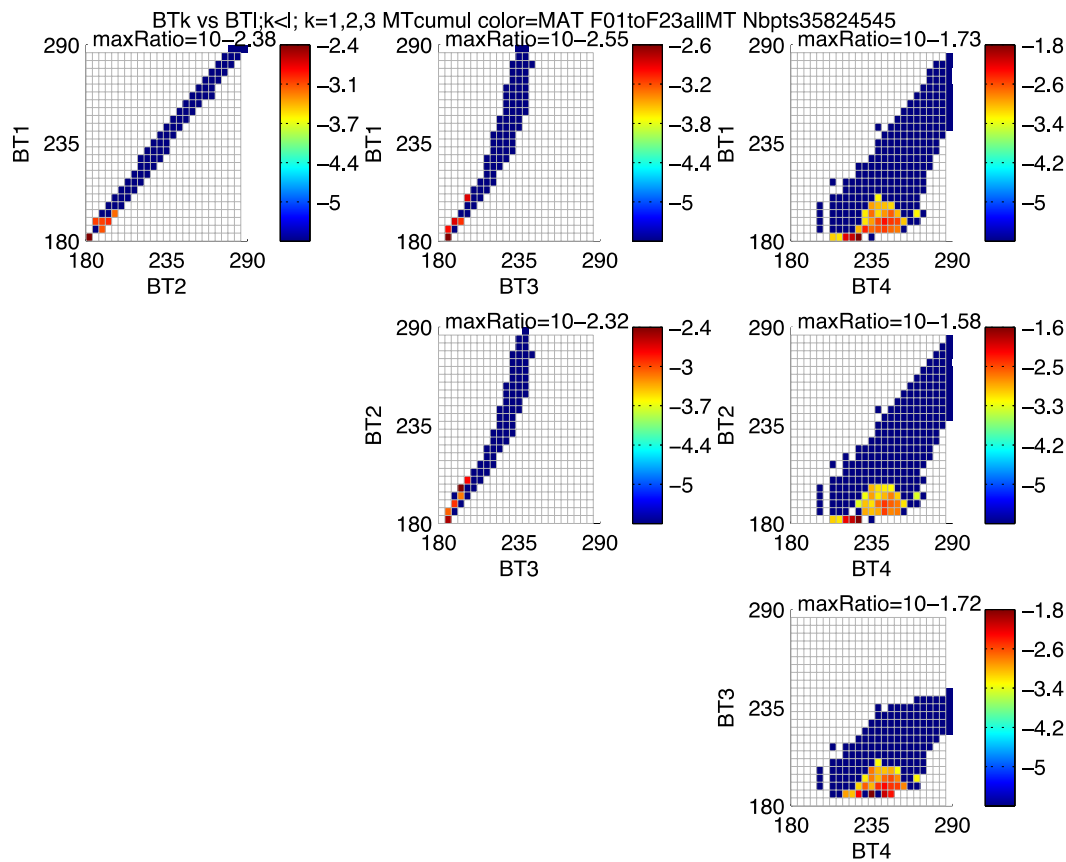
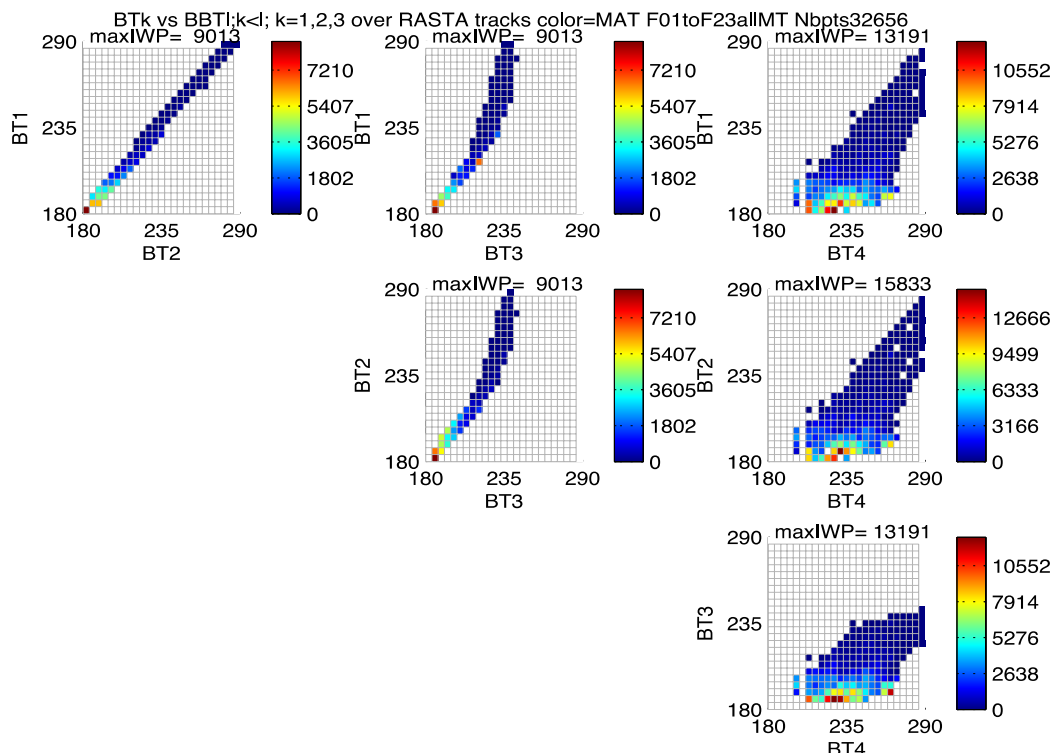


Figure3.c Ratios of RASTA observations in BT domains wr to MTSAT full BT images in log10 scale
→ the most observed area relatively to MTSAT overall density bins is a half-disk in BT4 WV channel ranging in 210-250K BT4 and the segment 180-200K in BT1,2,3



Figure

3d. IWP overall Max per MTSAT BT_{ij} bins. Max IWP reaches 9kg.m⁻² in BT12,13,23, Max(mean(IWPmax)) is 13.2kg.m⁻² in BT14 and 34 and even 15.8kg.m⁻² in BT24 domain

→ as expected, MaxIWP decreases linearly vs B_{ij}. In the three BT i,4 domains, the MaxIWP distribution follows the same pattern as for RASTA relative density.

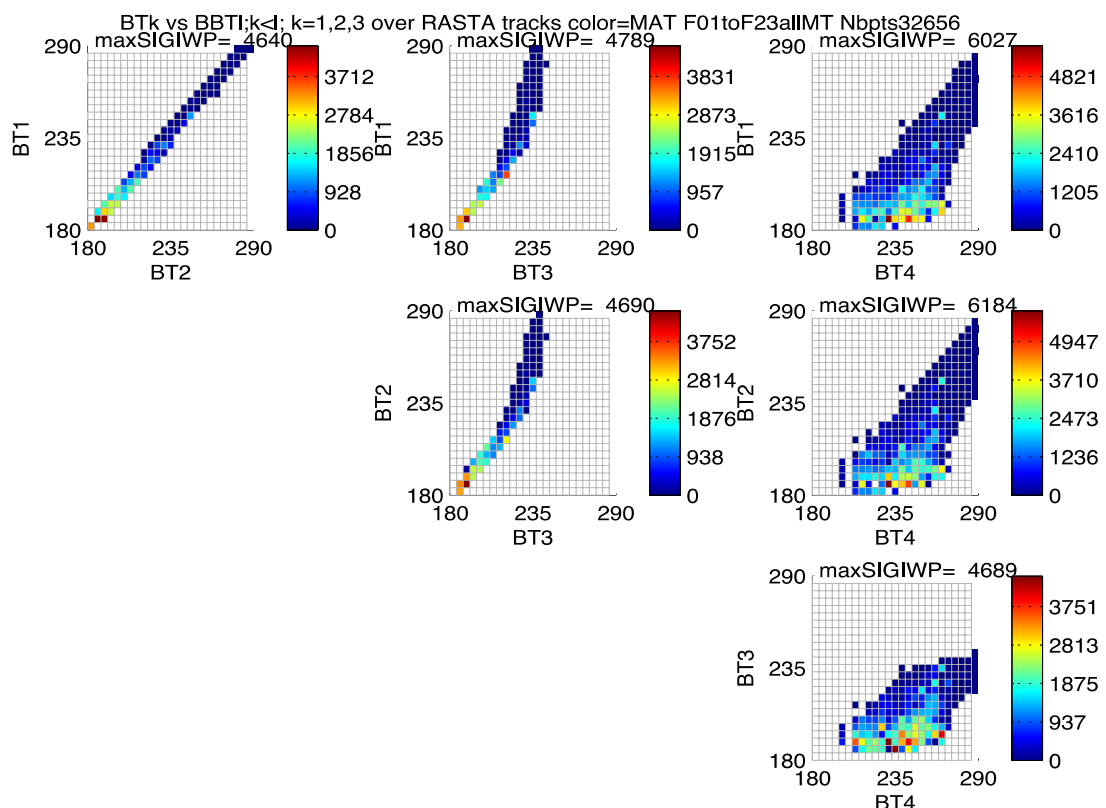


Figure 3e. Overall variance IWP per MTSAT BT bins. Variance can be as high as 6kg.m⁻² in BT 24. In BT12,13,23, maxIWP variance of 4.6kg.m⁻² is reached around 180K

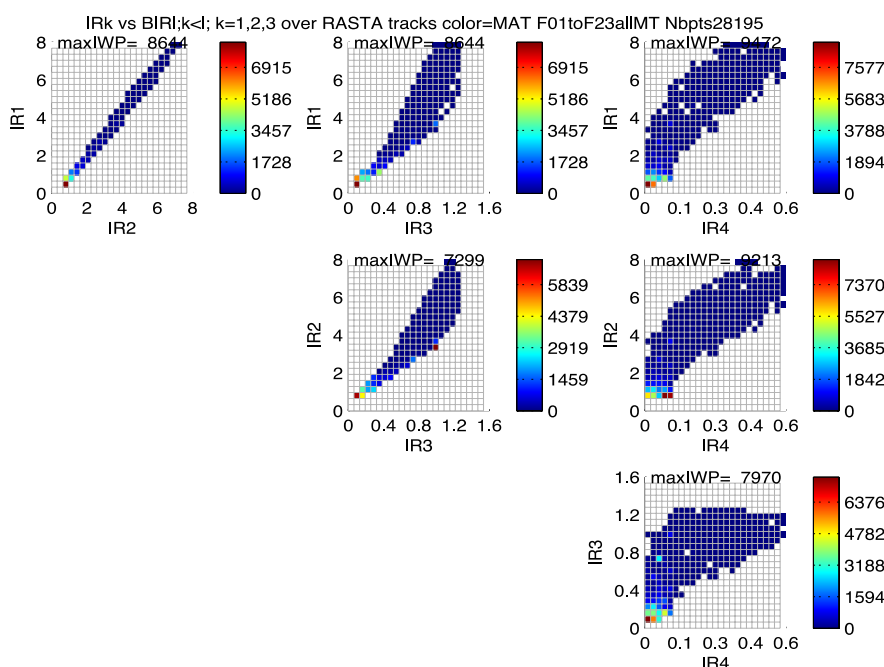


Figure 4. Overall mean IWP per IR bins

Second set of figures shows examples of MTSAT-RASTA Neural Network HIWP cells vs MTSAT Radiance1 at 10.8μm images and retrieved IWP images

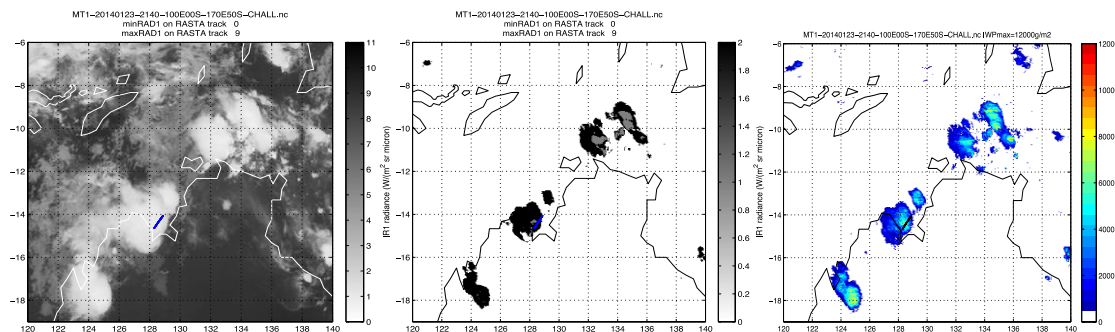


Figure 5. (left) MTSAT Radiance 10.8μm image, (middle) thresholded Rad1 image, (right) MTSAT-RASTA nnet IWP_levels image for F06MT27 2014/01/23 @ 21:55UTC in the ROI 120°,140°E 6°,19°S

Radiance 1 thresholds are : black R1<1.25, grey <0.9 W/m²/sr

IWP_levels color scale is : blue 1.7 - 3 kg/m², orange 3 - 4.5 kg/m², red 4.5 - 6.4 kg/m², black > 6.4 kg/m²

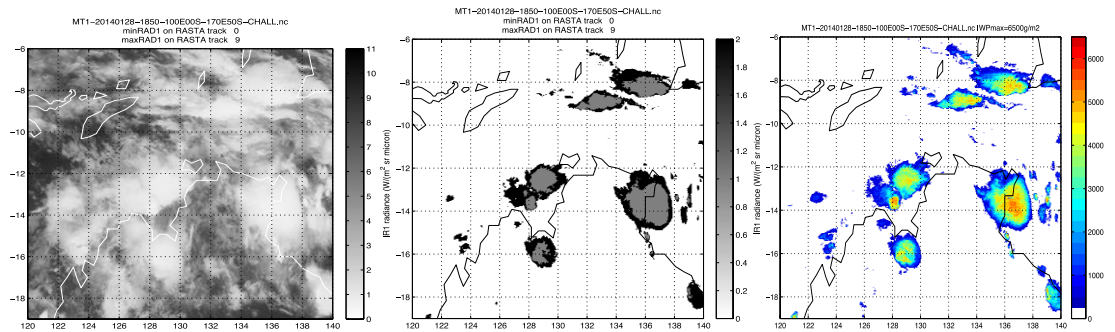


Figure 6. (left) MTSAT Radiance 10.8μm image, (middle) thresholded Rad1 image, (right) MTSAT-RASTA nnet IWP_levels image for F09MT05 2014/01/28 @ 18:50UTC in the ROI 120°,140°E 6°,19°S
IWP color scale : Yellow = 4000g/m²

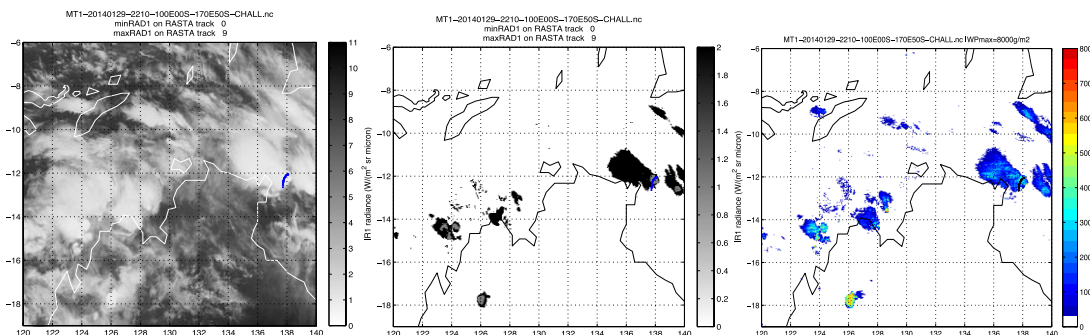


Figure 7. (left) MTSAT Radiance 10.8μm image, (middle) thresholded Rad1 image, (right) MTSAT-RASTA nnet IWP_levels image for F10MT29 2014/01/29 @ 22:25UTC in the ROI 123°,133°E 7°,16°S

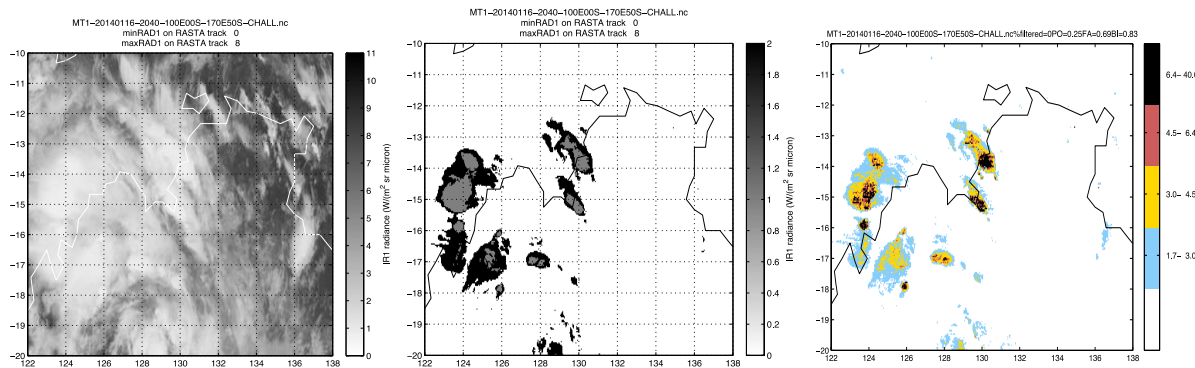


Figure 8. (left) MTSAT Radiance 10.8 μm image, (middle) thresholded Rad1 image, (right) MTSAT-RASTA nnet IWP_levels image for F02MT15 2014/01/16 @ 20:50UTC in the ROI 122°,138°E 10°,20°S

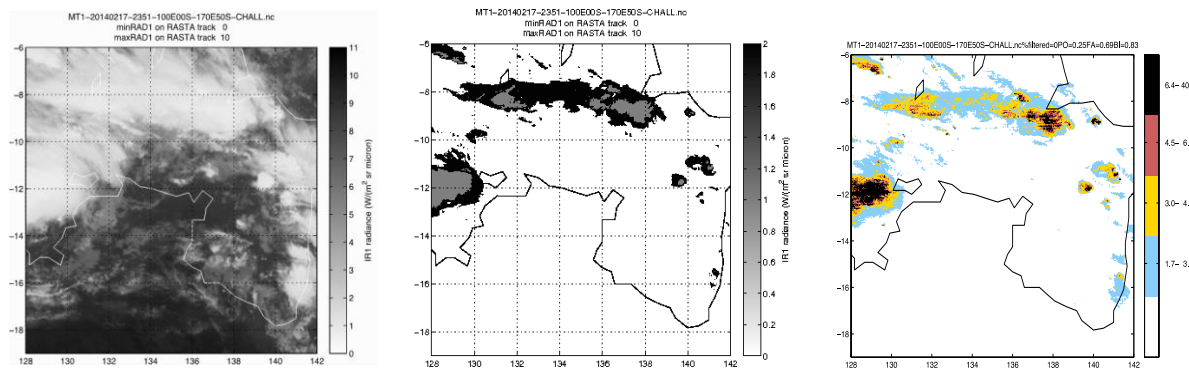


Figure 9. (left) MTSAT Radiance 10.8 μm image, (middle) thresholded Rad1 image, (right) MTSAT-RASTA nnet IWP_levels image for F22MT33 2014/02/18 @ 00:09UTC in the ROI 128°142°E 8°,19°S

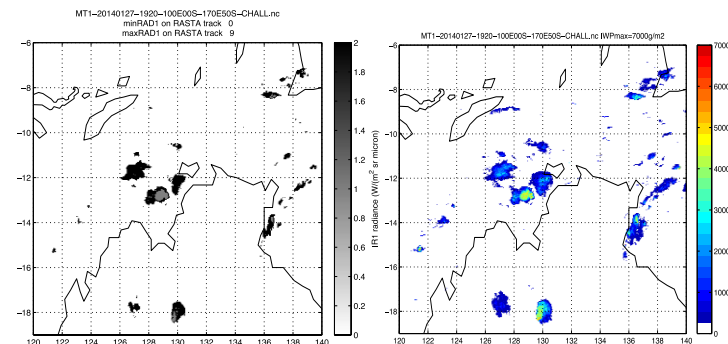


Figure 10 . (left) MTSAT Radiance 10.8 μm image, (center) thresholded Rad1 image, (right) MTSAT-RASTA nnet IWP_levels image for F08MT14 2014/01/27 @ 19:35UTC in the ROI 122°133°E 8°,20°S

Third set of figures illustrates NNET performances in training part

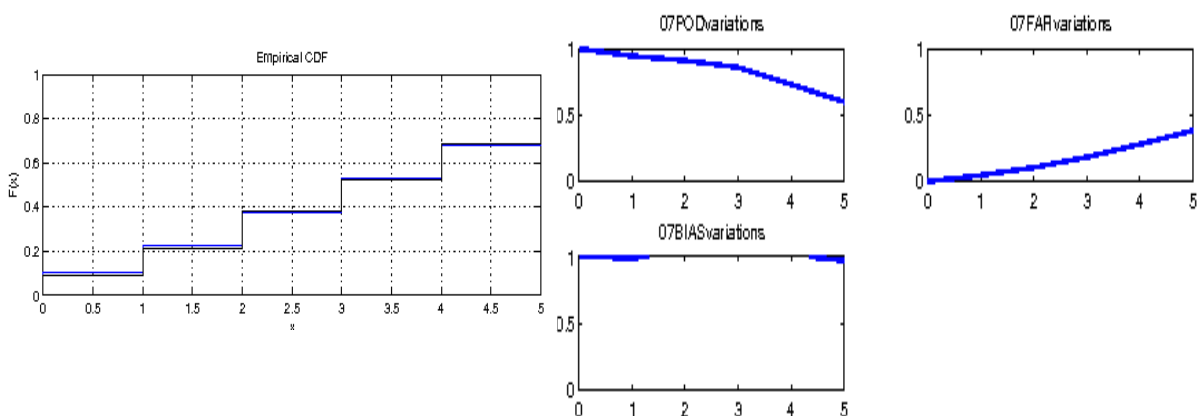


Figure 11.a (left) configuration#2 Training result for the empirical cumulated distribution function (ecdf) of IWP_levels Outputs (black) vs Targets (blue). Almost same ecdf for target and output is obtained

(right) POD, FAR, BIAS of Outputs vs Targets and IWP target distribution

Figure 12.a Config.#2 (top) Boxplot of IWP_level (Output – Target) over 235,000 training data points (bottom) Boxplots per IWP ranges : 0-1kg.m-2; 1-5kg.m-2; 5-40kg.m-2

- All 3 intervals give satisfactory results with average IWLevel difference less than 0.4 in absolute values, resp. -0.4; -0.1; 0.4
- Median IWP level equals 0 for all 3 intervals
- 50% of values are within : [-1 0]; [0 0]; [0 1] resp.
- 99% of diffs are within : [-2 0]; [-1 1]; [0 2] resp.

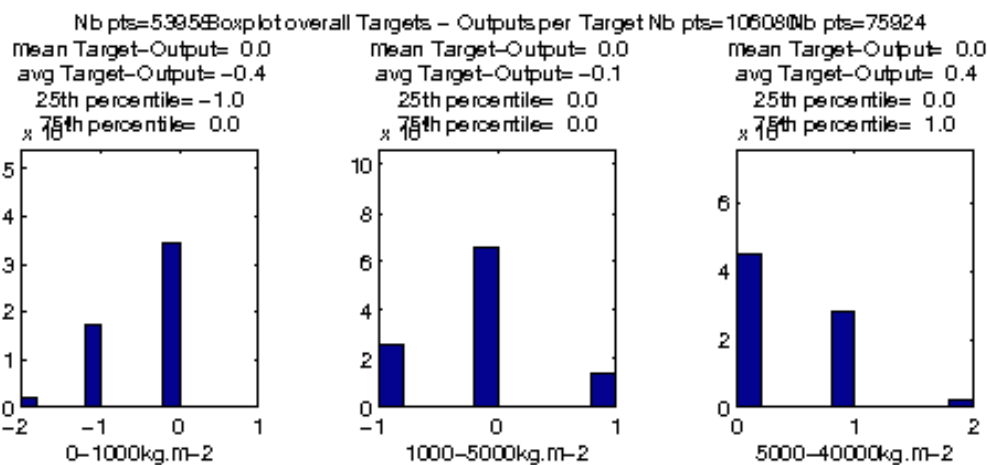


Figure 12. Same as Fig12.a except using Histogram ($\alpha_1=-0.48$ & $\alpha_2=0.6$ wr 4.5kg/m²)

→ NNET is well defined on center meta-class 1-5 kg.m-2. It overestimates beyond 5kg in 14% of cases and underestimates under 1kg in 23% of cases

Figure 13a. Config#1

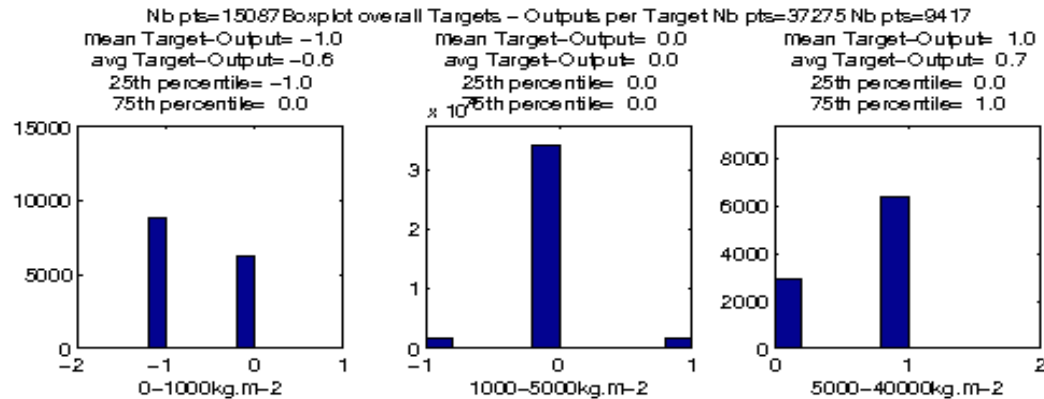


Figure 13.b Config.#1 Same as Fig13a except using Histogram.

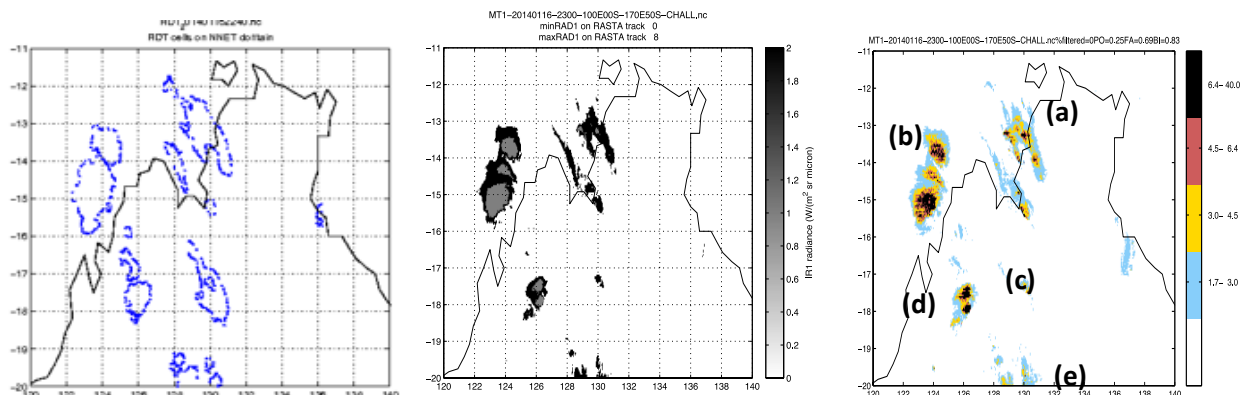
Comparison #1 : MTSAT-RASTA nnet vs RDT MTF during Darwin campaign

Fig 14. F02MT28 MTSAT-RASTAnnet-HIWP vs RDT cells comparison on 2014-01-16 23:00UTC on (120°,140°)E (11°, 20°)S. IWLevel intervals are : [1.7, 3[;[3,4.5[; [4.5,6.4[;[6.4,40[kg.m^-2

All cells are in agreement between the 3 sets, except RDT cell centered on (18°S,130°E) which does not appear neither in Radiance 1 nor in nnet result.

(left) MTF RDT lat-lon contour cells

(center) MTSAT Rad1 thresholded image with thresholds at 0.9 and 1.25 W.m-2.sr.s-1

(right) MTSAT-RASTAnnet cell detection image

Group (a) cells are detected in both radiance and IWLevel nnet

Group (b) is well detected with peak locations at same places in radiance and IWLevel

Group (c) southern part is not seen in both MTSAT thresholded and nnet image vs RDT

Group (d) is detected

Group (e) is detected

Comparison #2 : MTSAT-RASTA nnet vs AMSRE TRMM during Darwin campaign

Example#1 2014-01-30 F11MT35

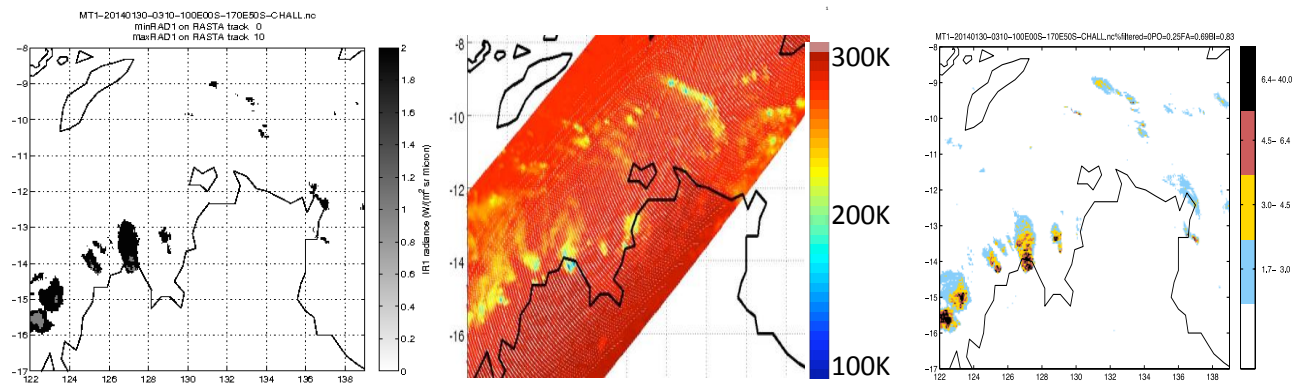


Figure 15. F11MT35 2014/01/30 @ 03:25UTC in the ROI 122°,140°E 8°,17°S

(left) MTSAT Rad1 thresholded image with thresholds at 0.9 and 1.25 W.m-2.sr.s-1

(center) TRMM BT @ 89GHz

(right) MTSAT-RASTAnnet cell detection image

→ Very good agreement between MTSAT-RASTA nnet and MTSAT thresholding

→ Group cells are seen in TRMM in yellow which corresponds to BT ~ - K and these

Example#2 2014-01-28 F09MT04

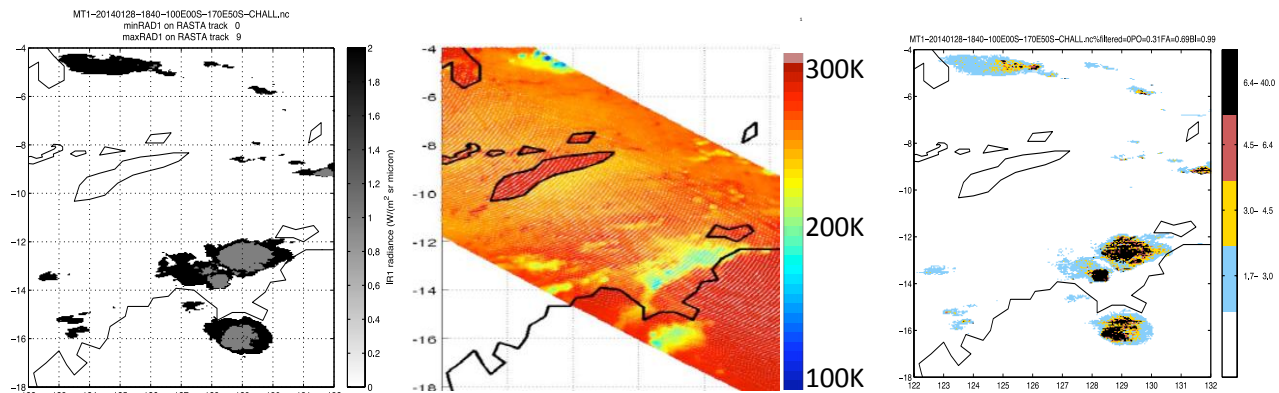


Figure 16. F09MT04 2014/01/28 18:40UTC in ROI 122°,132°E 4°,18°S

→ MTSAT Rad10.8 threshold and nnet are again in very good agreement

→ Main cells are consistent with TRMM BT image

Example#3 2014-01-21 F05MT46

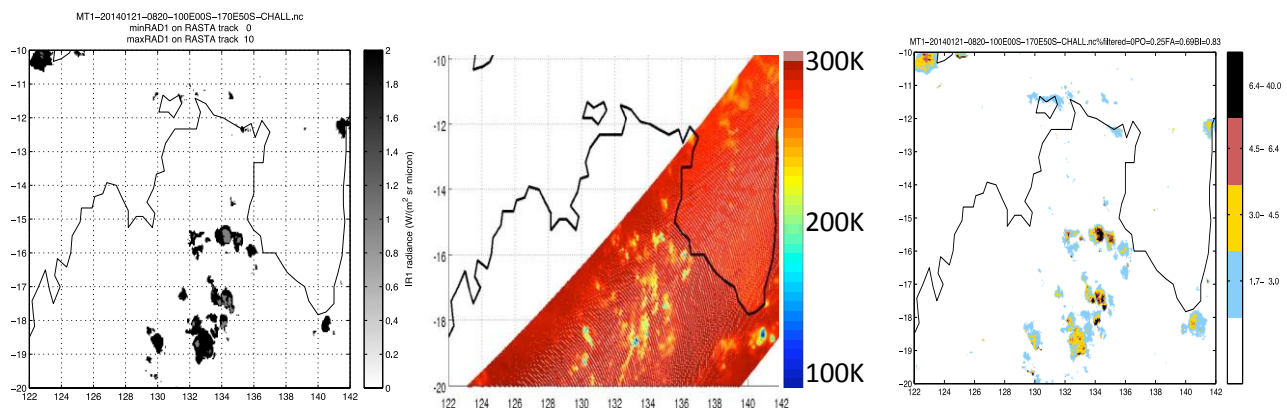


Figure 17. F05MT46 2014/01/21 08:20UTC in ROI (122°,142°)E (10°, 20°)S
(left) MTSAT Rad10.8mc thresholded at 0.9 and 1.25 W.m-2.sr-1.s-1

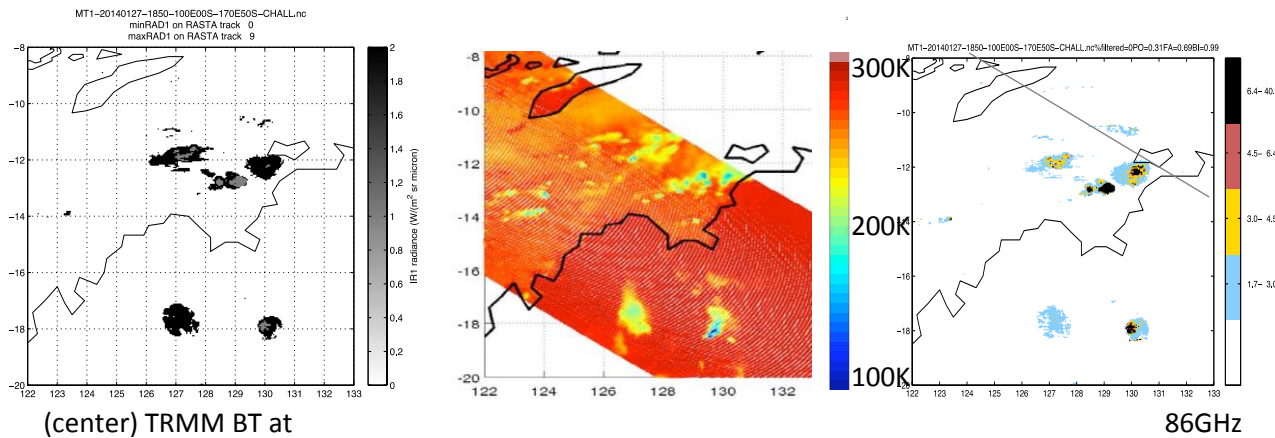


Figure 18. F08MT11 2014/01/27 18:50UTC in ROI (122°,133°)E (8°, 20°)S
(left) MTSAT Rad10.8mc thresholded at 0.9 and 1.25 W.m-2.sr-1.s-1
(center) TRMM BT at 86GHz on time range
(right) MTSAT-RASTA nnet for IWP > 1.7 kg.m-2

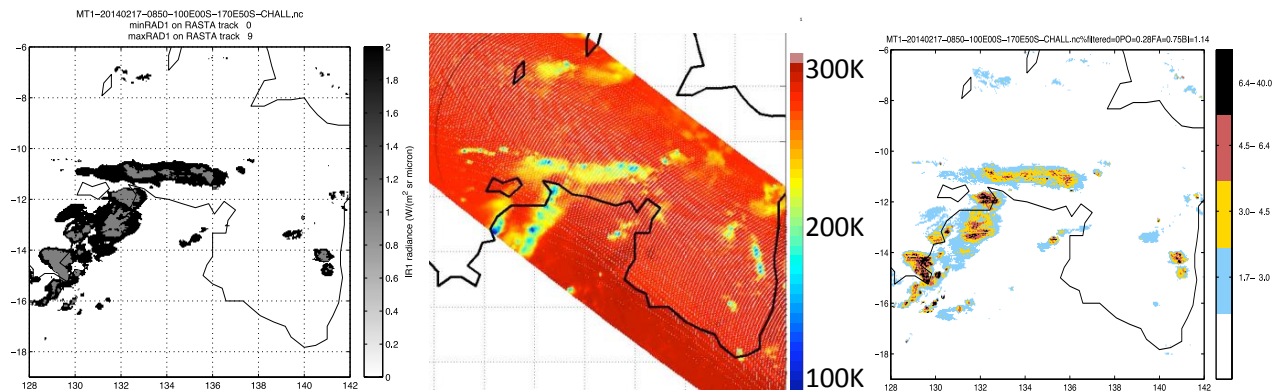


Figure 19. F21MT33 2014/02/17 08:20UTC in ROI (128°,142°)E (6°, 19°)S
(left) MTSAT Rad10.8mc thresholded at 0.9 and 1.25 W.m-2.sr-1.s-1
(center) TRMM BT at 86GHz on time range UTC
(right) MTSAT-RASTA nnet for IWP > 1.7 kg.m-2

The orthogonal feature located at [11°,16°]Sx[132°,138°]E is well detected by the nnet.
The upper cells with BT ~ K is only partly detected.

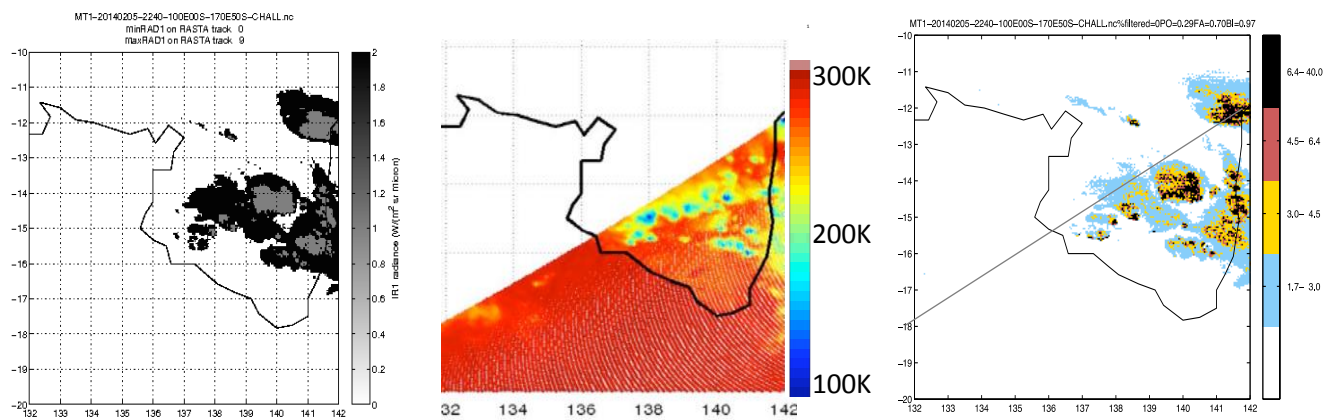


Figure 20. F15MT15 2014/02/05 22:55UTC in ROI (132°,142°)E (10°, 20°)S

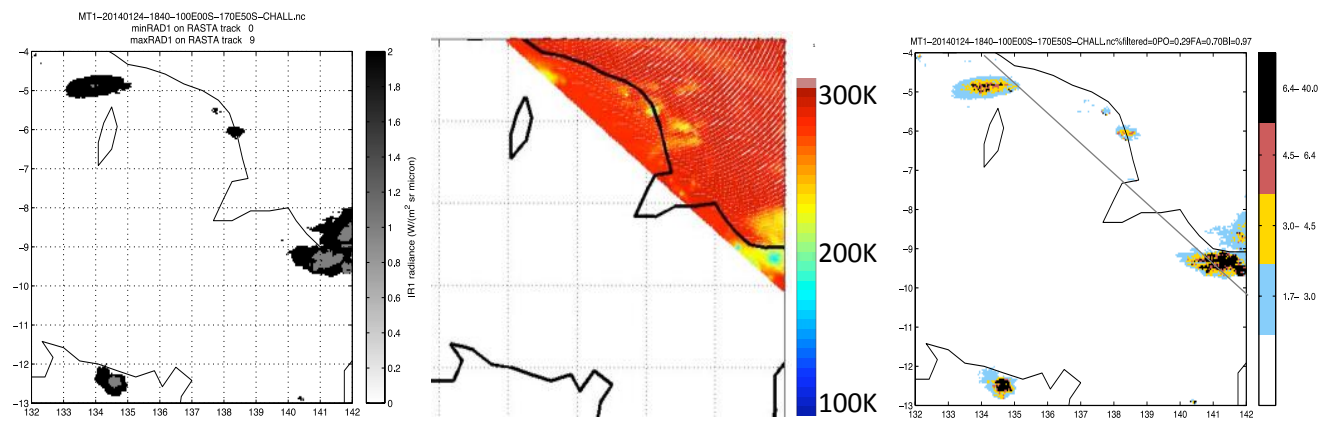


Figure 21. F07MT10 2014/01/24 18:55UTC in ROI (132°,142°)E (4°, 13°)S